Improved Backscatter Correction Model for High Attenuation Gamma-ray Tomography Measurements

R.B. Spelay[1]*, S.A. Hashemi[1], R.S. Sanders[2], B.T. Hjertaker[3]

[1] Saskatchewan Research Council, Pipe Flow Technology Centre™, Saskatoon, SK, Canada
[2] University of Alberta, Dept. Chemical and Materials Engineering, Edmonton, AB, Canada
[3] University of Bergen, Dept. Physics and Technology, Bergen, Norway

*Email: ryan.spelay@src.sk.ca

ABSTRACT

In this study a state of the art Gamma-ray Tomography unit (GRT) at the Saskatchewan Research Council's (SRC) Pipe Flow Technology Centre™ was used to measure the solids concentration distributions of high density, high attenuation clay/water/sand slurries in 4 in. (100 mm) diameter recirculating pipe loop. The presence of neighbouring radiation sources on the GRT results in a scattered radiation contribution to the total intensity measured at each detector. The backscattered radiation decreases the signal-to-noise ratio of the measured radiation intensity and introduces error in the measured tomography data and the reconstructed tomograms (Maad et al., 2008). Because of the high attenuation of the materials being measured, in some cases the backscatter contribution was a significant fraction of the total radiation measured at each detector. To correct for the scattered radiation contribution in the measurements, a test campaign was undertaken to characterize and model the backscattering for the GRT unit at SRC. The scattered radiation was measured experimentally from empty pipe, water filled pipe and a number of flowing clay/water/sand slurry tests at mixture densities ranging from 1206·kg/m³ to 1580·kg/m³. A semi-empirical backscatter correction model has been developed which allows the backscattered contribution at each detector to be calculated iteratively based on the measured uncorrected attenuated radiation intensity.

Keywords backscatter, correction, gamma-ray tomography, slurry

Industrial Application Mining and Mineral Processing, Slurry Pipeline Research

1 INTRODUCTION

Mineral processing slurries are complex mixtures that can contain particles with a broad size and/or density range (e.g. mineral solids, silica sands, clays). From the extraction of the valuable minerals to the final placement of the tailings, slurry pipeline transport is a significant mode of moving these materials throughout the mine and mill. In order to better understand the flow behaviour of these slurries, so that reliable and efficient transport systems can be designed, knowledge of the solids concentration distribution in pipeline flows under different operating conditions is required so that predictive models can be developed. Gamma-ray tomography is a non-intrusive measurement tool that can be used to accurately measure these solids concentration distributions.

Gamma-ray tomography involves the use of radioisotopes (e.g. Cs-137, Am-241) which through radioactive decay emit gamma-ray radiation at a specific energy level (Cs-137 at 660 keV, Am-241 at 59.5 keV). The radioisotope is held in sealed source containers and the radiation emitted is directed through a measurement volume and collimated. Measurement of the transmitted (unabsorbed) radiation intensity is made using detectors. The ratio of the measured intensity (at the specific energy level of interest) relative to the unattenuated intensity can be related to the density or volumetric concentration of the materials present in the measurement volume. For slurries, from the knowledge of the attenuation coefficients of the solid and liquid phases and the path lengths of the measurement volume, the solids concentration distribution in the pipe can be determined.

The gamma rays produced by the decay of the radioactive isotope in the source container can undergo a number of Compton scattering processes before entering the detector material. One of the following three phenomena can occur:

1. The radiation is absorbed by the material in the measurement volume.
2. The unabsorbed radiation is transmitted and measured at the detectors.
3. The radiation is reflected (or backscattered) by either the absorbing material, pipe, or interfering material of construction of the GRT.

The radiation intensity measured at the detectors is a combination of both the incident radiation not absorbed by the measurement material as well as the Compton backscattering radiation which has been reflected from the material in the measurement volume and the GRT. The amount of backscattering radiation is a function of the geometry of the GRT as well as the materials of construction and the material being measured. Since gamma-ray sources emit radiation isotropically, the amount of backscattering and the true attenuated radiation are statistically related and can be measured.

Unlike traversing gamma-ray densitometers which only use a single source and detector arrangement to produce a vertical chord averaged solids concentration distribution over the pipe cross-section (Spelay, 2007), the gamma-ray tomography (GRT) unit at the SRC's Pipe Flow Technology Centre™ employs the simultaneous operation of 5 sources and 5 pentants to produce a two-dimensional tomogram of the solids concentration distribution in the pipe cross-section. The use of only a single source and detector in the traversing gamma-ray densitometer requires no secondary (Compton backscattering) correction. However, the presence of multiple sources on the GRT (that operate simultaneously) results in backscattered radiation measured at each detector from the neighbouring sources (those not located directly across from it). The transmitted radiation is easily measured, but determining the fraction of the measured radiation at each detector that is due to backscattering is far more complex (Tjugum et al., 2003). If left uncorrected, including the backscattered radiation contribution in the measured intensities can result in uncertainty and error in the reconstructed tomogram.

2 BACKGROUND

2.1 SRC GRT Unit

The SRC GRT unit is based on a similar design to the University of Bergen (UiB) GRT equipment (Johansen et al., 1996). The SRC GRT consists of 5 x 500 mCi Am-241 (Americium-241) sources each located at the vertex of a regular pentagon (at 0°, 72°, 144°, 216°, 288°). Located directly across from each source along a pentagonal face is the corresponding pentant (bank of detectors). Each pentant consists of a bank of CdZnTe detector elements. Figure 1 shows a schematic and illustration of the GRT unit at the SRC.

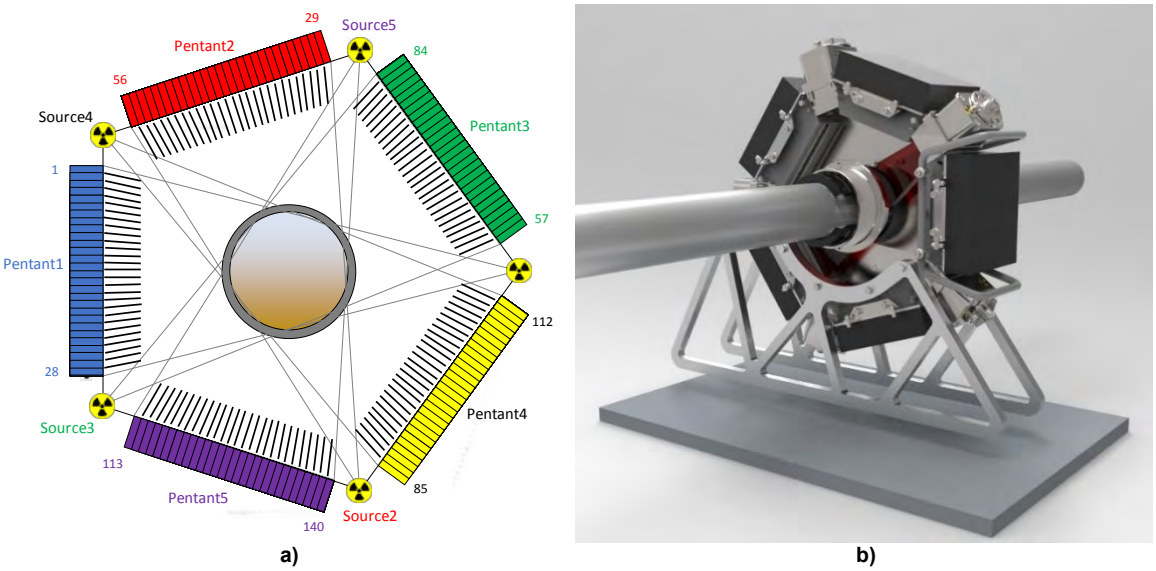

Figure 1. Schematic and illustration of the SRC GRT unit:
a) Arrangement of the sources, measurement volume, collimator blades and pentant (detectors),
b) Cut-away illustration of the radiation beam path.

The detecting elements on each pentant consist of 7 crystals. Each crystal is composed of a matrix of elements that is 16 pixels (wide) by 8 pixels (high), resulting in a detecting crystal array composed of 896 discrete sensing pixels (16 x 8 x 7). In total there are 4480 individual detecting pixel elements for all five pentants on the GRT. To reduce the amount of backscattered radiation, the radiation beam from each source is physically collimated at the pentant. Lead collimator blades (1 mm thick) were installed in front of the detector elements to focus the radiation from the source directly across from each detector and limit off-angle scattered radiation. The collimator blades are located such that four adjacent columns of pixels (4 x 8 pixels) are averaged to produce 28 independent detector readings from each pentant (140 total detectors on all five pentants of the GRT). Figure 2 shows the location of the collimator blades (red lines), and the collimation of the pixels to produce 28 detectors per pentant.

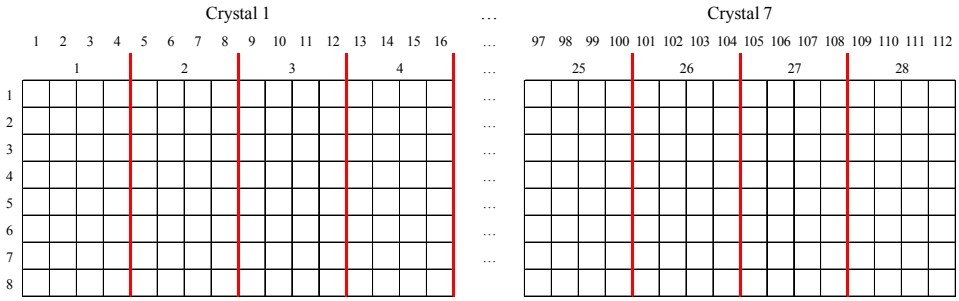

Figure 2. Schematic of the pixel collimation into detectors on each pentant.

The measured radiation intensity from each pixel can be averaged with adjacent pixels to produce any number of virtual detectors. Due to the high attenuation of the materials being measured, and to limit the error on the measured results, the unit was configured to output 28 detectors per pentant (140 total detectors). Each source (S) is located directly across from a pentant (P) containing 28 detectors. Table 1 details the detector numbers corresponding to each source and pentant as well as the neighbouring sources adjacent to each pentant on the SRC GRT Unit.

Table 1. Source, pentant and detector arrangement on the SRC GRT unit.

Source	Pentant	Detectors	Neighbouring Sources
S1	P1	1-28	S3, S4
S2	P2	29-56	S4, S5
S3	P3	57-84	S5, S1
S4	P4	85-112	S1, S2
S5	P5	113-140	S2, S3

Data is collected from the unit using the ethernet protocol and LabView data acquisition software from National Instruments. The unit can acquire data at frequencies as fast as 100 Hz (10 ms). However, due to the high attenuation of the materials that were tested in this study, and because the error in the measured intensity from each detector is proportional to the square root of the counts acquired over the measurement time, 30 x 10,000 ms data sets were acquired (300 s or 5 min) for all backscattering measurements presented in this study.

2.2 Backscatter

The transmission of radiation through attenuating materials between a source and a detector can be expressed by the Beer-Lambert Law (Shook & Roco, 1991, Ch10, pp. 219-223). The expression by Maad et al. (2008) in Equation 1 shows the total contribution of both absorbed and scattered radiation measured at each detector.

$$I_{T,i} = BI_{0,i}e^{-\sum \mu_j x_j} + I_{S,i} \quad (1)$$

Where:

$I_{T,i}$ = attenuated radiation intensity at detector *i* (Hz)

$I_{0,i}$ = unattenuated incident radiation intensity at detector *i* from the source directly opposite (Hz)
$I_{S,i}$ = scattered contribution at detector *i* from the four other sources (Hz)
B = build-up factor accounting for forward scatter from the transmission source (~ 1)
μ_j = attenuation coefficient of material *j* in measurement volume (cm^{-1})
x_j = path length of material *j* in measurement volume (cm)

The scattered radiation at detector *i* ($I_{S,i}$) is the sum of the contributions from each of the four sources not directly opposite the detector (*n* = 1 to 4). This is shown below in Equation 2.

$$I_{S,i} = \sum_{n=1}^{4} I_{S,n} \tag{2}$$

Therefore, the scattered radiation from each source ($I_{S,n}$) can be measured systematically by using only one active source at a time and mechanically closing the shutters on the remaining sources (Maad et al., 2008). This can be repeated for each source and summed using Equation 2 to get the total scattered radiation contribution at each detector. However, since the scattered radiation is a function of the attenuating material being measured (i.e. material density and path length), the objective of this study is to measure the scattered radiation for slurries with a range of densities (relevant to the mining and mineral processing industries) and develop a predictive correlation which provides a means to correct for this contribution in the measured signal.

3 EXPERIMENTAL METHOD

3.1 System

A schematic of the SRC 4 in. (100 mm) diameter recirculating pipe loop employed in this study is shown in Figure 3. The GRT is mounted on a horizontal, transparent, 4 in. (100 mm) diameter section of Schedule 40, CPVC (Chlorinated Polyvinyl Chloride) pipe located on the return leg of the pipe loop. CPVC pipe was chosen for the pipe spool because it is low density and thus does not result in a significant attenuation of the measured signals (relative to steel pipe for example). The GRT is located far downstream from any bends or fittings (over 200 pipe diameters) ensuring the measurement of fully developed solids concentration distributions at the unit. For more information on the operation of recirculating pipe loops at the SRC Pipe Flow Technology Centre™, Spelay et al. (2016) and Spelay et al. (2017) provide thorough explanations.

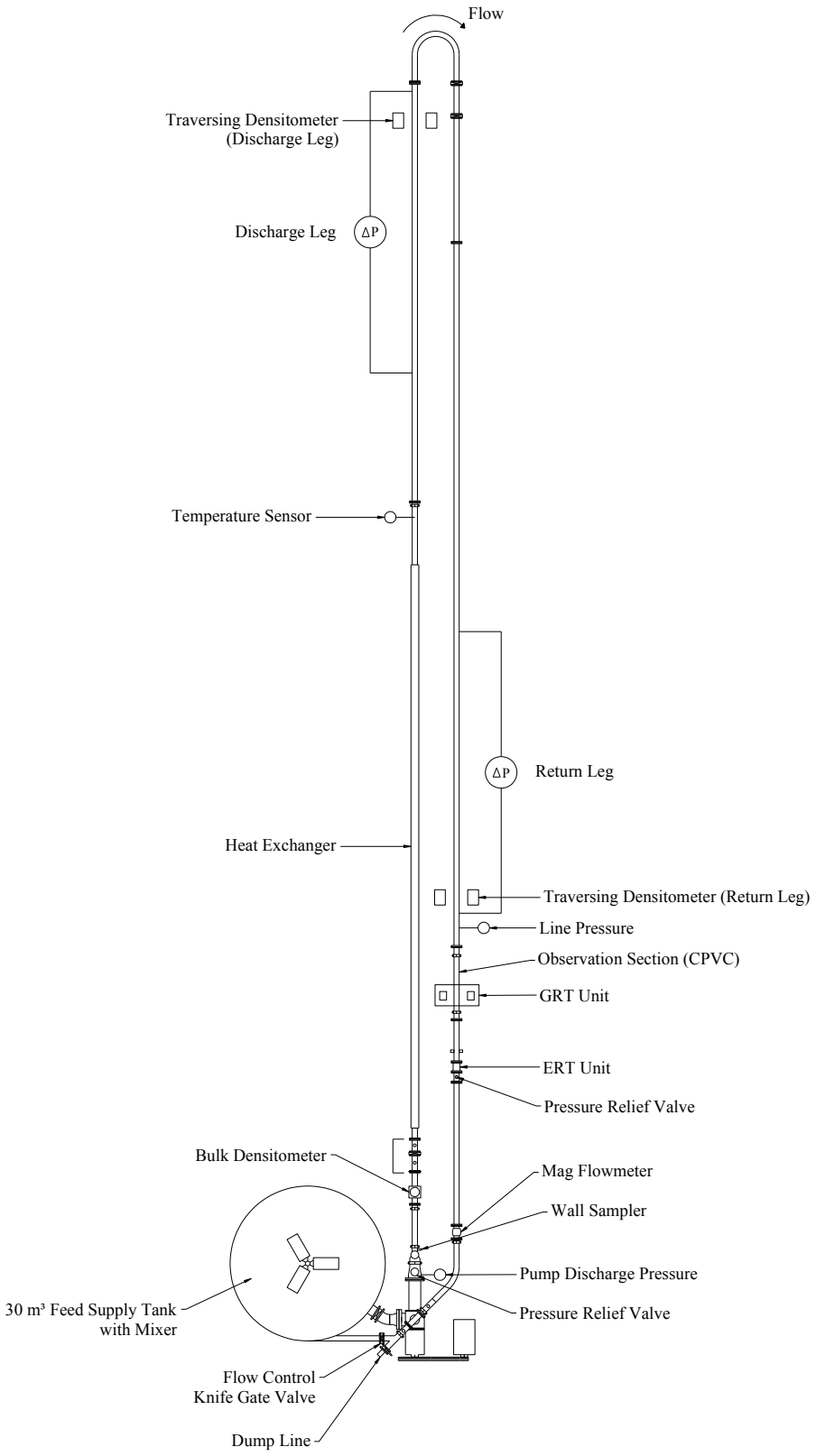

Figure 3. Schematic of the SRC 4 in. (100 mm) diameter recirculating pipe loop.

3.2 Materials

The attenuated and the backscattered radiation are functions of the unattenuated radiation intensity, geometry of the GRT, materials of the GRT construction and the density and thickness (attenuation) of the materials being tested in the unit. For a given GRT setup, the amount of backscattering relative to

the attenuated intensity measured at the detector increases with an increasing attenuated signal (Mosorov et al., 2011). Higher density materials (which absorb more gamma radiation) also result in more backscattering. Measurements were taken on the following materials in order to develop a predictive correlation:

a) Empty Pipe;
b) Water filled pipe;
c) Homogeneous clay-water slurries with solids concentrations of 12.5%v, 15%v, 17.5%v;
d) Each carrier fluid (CF) slurry in (c) with 5%v, 10%v and 20%v sand additions; and
e) For some of the tests additional measurements were taken on the 20%v slurry in (d) that were dispersed with a chemical addition of Tetrasodium Pyrophosphate (TSPP) to reduce the yield stress of the mixture.

Table 2 shows the density range of the slurries described above and tested in the study. Tests were conducted with empty pipe, water filled pipe and on concentrated slurries composed of kaolin clay (Pioneer kaolin clay), silica sand (Lane Mountain 125 and Granusil 4020) and water to represent industrial mineral tailings slurries. During backscattering tests for slurries with coarse settling sand, the pipeline system was operated at a velocity in turbulent flow above the deposition velocity of the slurry (the velocity at which a stationary bed of solids accumulates on the bottom wall of the pipe) such that the solids concentration distribution of the slurry was uniform (i.e. homogeneous across the pipe cross-section). This was confirmed by viewing the live/online reconstructed tomograms from the GRT unit at the operating condition of interest.

Table 2. Densities of mixtures (in kg/m³) tested during backscattering test program

Test	Test				
	1	2	3	4	5
Empty Pipe	N/A	N/A	N/A	N/A	N/A
Water	998	999	998	998	998
CF	1206	1243	1244	1288	1282
CF+5%v Sand	1280	1316	1331	1353	1355
CF+10%v Sand	1360	1399	1395	1426	1429
CF+20%v Sand	1511	1533	1539	1566	1580
CF+20%v Sand + TSPP	--	--	--	1566	1579

Saskatoon city tap water was used for the water tests and in the preparation of all slurries tested in this study. The density of water (as a function of operating temperature) was determined from the tabulated values for pure water in the literature (Perry & Green, 1997, Ch2, p2-91). The density of each slurry was determined by thoroughly washing representative samples of slurry taken from the pipeline over a 325 mesh (45 µm) sieve to separate the coarse sand from the fine clays. Drying and weighing of the separated sand and clay solids (and with measurement of the original sampled slurry mass) allowed the mass concentration of each phase (clay, sand and water) to be determined and thus the density of the whole slurry to be calculated. The relationship used to calculate the slurry density is provided below in Equation 3. The particle densities of the clay and sand were determined by a solids in water volume displacement technique prior to the study (i.e. pycnometry), and were found to be 2646 kg/m³ and 2650 kg/m³, respectively.

$$\rho_{mixture} = \left(\frac{C_{m,clay}}{\rho_{clay}} + \frac{C_{m,sand}}{\rho_{sand}} + \frac{C_{m,water}}{\rho_{water}} \right)^{-1} \quad (3)$$

Where:

$\rho_{mixture}$ = density of the mixture (kg/m³)
ρ_i = density of each phase in the mixture (kg/m³)
$C_{m,i}$ = mass concentration of each phase

Similarly, the volumetric concentration of each phase in the mixture (how the slurries are specified and reported in Table 2) can be determined from Equation 4.

$$C_{v,i} = C_{m,i}\frac{\rho_{mixture}}{\rho_i} \quad (4)$$

For the water, sand and clay type materials that were tested in this study, and that makeup most industrial mineral processing slurries, the attenuation coefficients were found to be directly proportional to their density. The relationship provided in Equation 5 was produced from measuring homogeneous clay/water slurries of known density in the GRT. The attenuation coefficient of the mixture was calculated from the measured intensities and the calculated path lengths from tests with water. The correlation provides an accurate prediction of the attenuation coefficients for the 59.5 keV Am-241 gamma radiation as a function of the material density.

$$\mu = 0.0002711\rho - 0.06453 \quad (5)$$

Where:

μ = attenuation coefficient of the material (cm^{-1})
ρ = density of the material (kg/m^3)

Table 3 shows the attenuation coefficients determined for the different materials of interest in this study.

Table 3. Attenuation coefficients for the different materials tested in the study

Material	Density, ρ (kg/m³)	Attenuation Coefficient, μ (cm^{-1})
Water	998	0.2060
CPVC Pipe	1560	0.3584
Kaolin Clay	2646	0.6529
Silica Sand	2650	0.6539

3.3 Backscattering Test Procedure

In order to determine the backscatter contribution from each source (at each detector), the following measurements were taken:

a) No sources installed (to obtain a measure of the background radiation intensity); and
b) No pipe with one source installed at a time on the unit (to get the true unattenuated intensity at each detector with no backscattering).

The following measurements were taken with all of the sources installed on the GRT:

c) All shutters open (to visualize the flow to see if the solids concentration distribution was uniform at the chosen operating velocity for the settling slurry tests); and
d) All shutters closed (to obtain a measure of the closed shutter intensity contribution from the source located directly across from each detector).

The following measurements were made with only one source shutter open at a time and with the rest of the source shutters closed:

e) S1 shutter open - S2, S3, S4, S5 shutters closed;
f) S2 shutter open - S1, S3, S4, S5 shutters closed;
g) S3 shutter open - S1, S2, S4, S5 shutters closed;
h) S4 shutter open - S1, S2, S3, S5 shutters closed; and
i) S5 shutter open - S1, S2, S3, S4 shutters closed.

A direct measurement of the backscattering cannot be obtained since closing the shutter on a source does not completely eliminate the radiation measured at the detector directly across from it. To calculate the backscatter intensity contribution, the closed shutter intensity measured for each detector

(in step (d)) was subtracted from each of the neighbouring source intensity measurements with a single source shutter open (steps (e) to (i)). The sum of the contributions from each of the four neighbouring sources is the true backscattering contribution at each detector (i.e. the backscattering at the detectors of pentant 1 (located directly across from source 1) is the sum of the differences between measurements (f) and (d), (g) and (d), (h) and (d) and (i) and (d)). No contribution for source 1 is included since it is directly across from pentant 1 and cannot backscatter radiation to those detectors. The backscattering for the detectors on the other pentants (P2 to P5) were calculated in a similar manner. In all calculations measurements were corrected for the background radiation measured in step (a).

4 RESULTS AND DISCUSSION

4.1 Backscatter Measurements

Figure 4 shows plots of the ratio of the measured scattered intensity to the attenuated intensity (the transmitted intensity using one source at a time) for the Test 5 (refer to Table 2) empty pipe, water, carrier fluid (clay/water slurry) and carrier fluid (clay/water slurry) with 20%v sand mixture. The contribution of the backscattered radiation from each source at each detector can be seen from the coloured fraction of the corresponding source on the figures (S1 = blue, S2 = red, S3 = green, S4 = yellow, S5 = purple). Refer to Figure 1 and Table 1 for more information on the sources that are across from and adjacent to each detector.

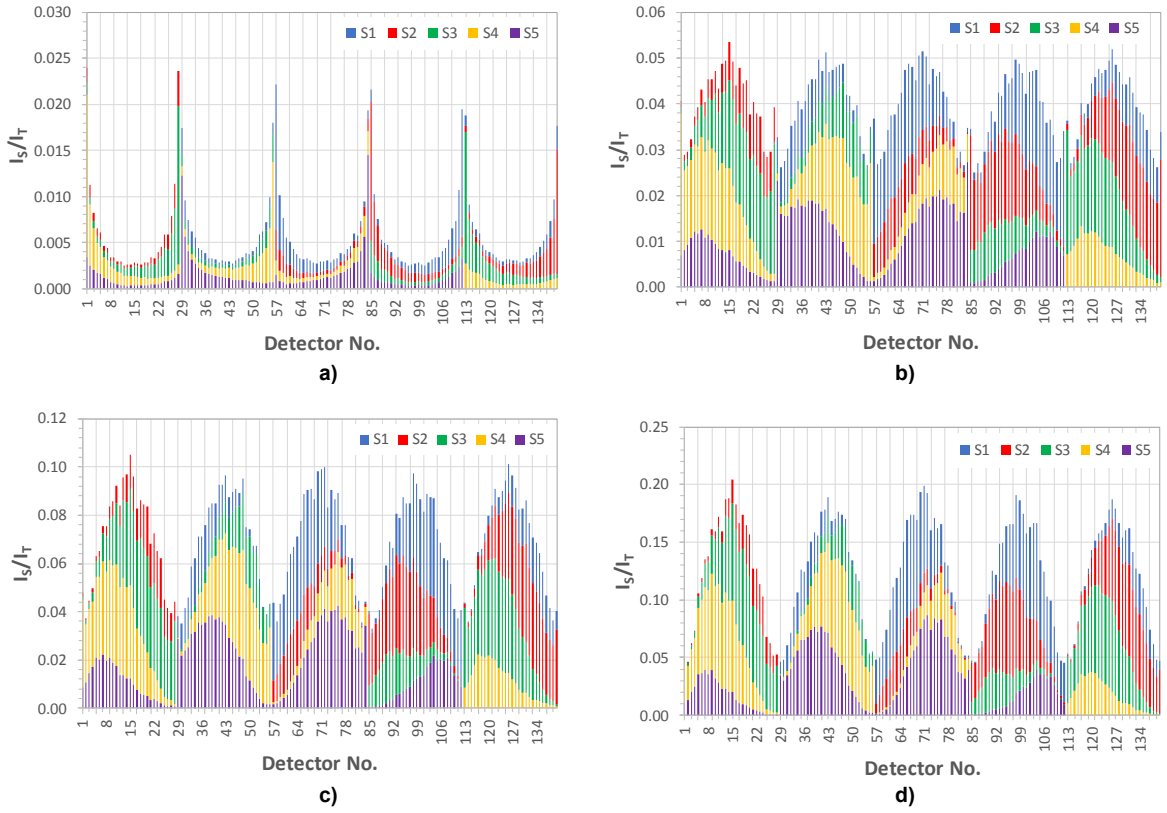

Figure 4. Ratio of scattered to attenuated radiation intensity from the neighbouring sources at each detector: a) Empty Pipe, b) Water (998 kg/m³), c) Clay/Water Slurry (1282 kg/m³), d) Clay/Water/Sand Slurry (1580 kg/m³).

The largest backscattering contribution for a detector comes from the two sources directly adjacent to the pentant on which it is located (e.g. for detectors 1-28 on pentant 1 across from source 1, sources 3 and 4 contribute the most backscattering). For the empty pipe measurements in Figure 4a, the backscattering is most significant for the end detectors nearest the edge of the pentant (since this is where the pipe is the thickest and the most attenuation occurs). The overall backscattering on the remaining detectors in the middle of the pentant is quite low and less than 0.5% of the attenuated intensity. However, comparison with Figures 4b to 4d for the tests with water and slurry, the backscattering increases with increasing material density and attenuation. For the most concentrated

slurries tested (1580 kg/m³), the maximum fraction of backscattered intensity was nearly 20% of the measured attenuated intensity. For tests where the pipe was full (with water or slurry), the maximum backscattering occurs near the middle of the pentant (middle of the pipe) where the longest path lengths and greatest attenuation exist. This is in agreement with the results of Mosorov et al. (2011). If left uncorrected, the inclusion of the backscattering contribution (as high as 20%) in the attenuated intensities could lead to significant errors in the reconstructed tomogram.

4.2 Backscatter Correction Correlation

The density of attenuating material between the source and detector can be determined using the Beer-Lambert law and the ratio of the attenuated to the unattenuated radiation intensities measurements. Likewise, the amount of backscattering from the neighbouring sources can also be determined using a similar approach. Figure 5 shows a plot of the normalized backscattering intensity (plotted as the natural logarithm of the ratio of the backscattering intensity to the attenuated or transmitted intensity, $-ln(I_S/I_T)$, versus the total attenuation along the path length, $\mu_T x_T$. The total attenuation is defined as the sum of the products of the attenuation coefficient (μ_j) and the path length (x_j) for each material in the measurement volume between the source and detector of interest. In this study the total attenuation along a given path length is the contribution from the water or solids (clay or sand) in the pipe and the thickness of the pipe wall along that path. Data is provided in Figure 5 for the backscattering measurements taken for all of the tests conducted with empty, water filled and slurry filled pipe as detailed in Table 2 (4480 data points).

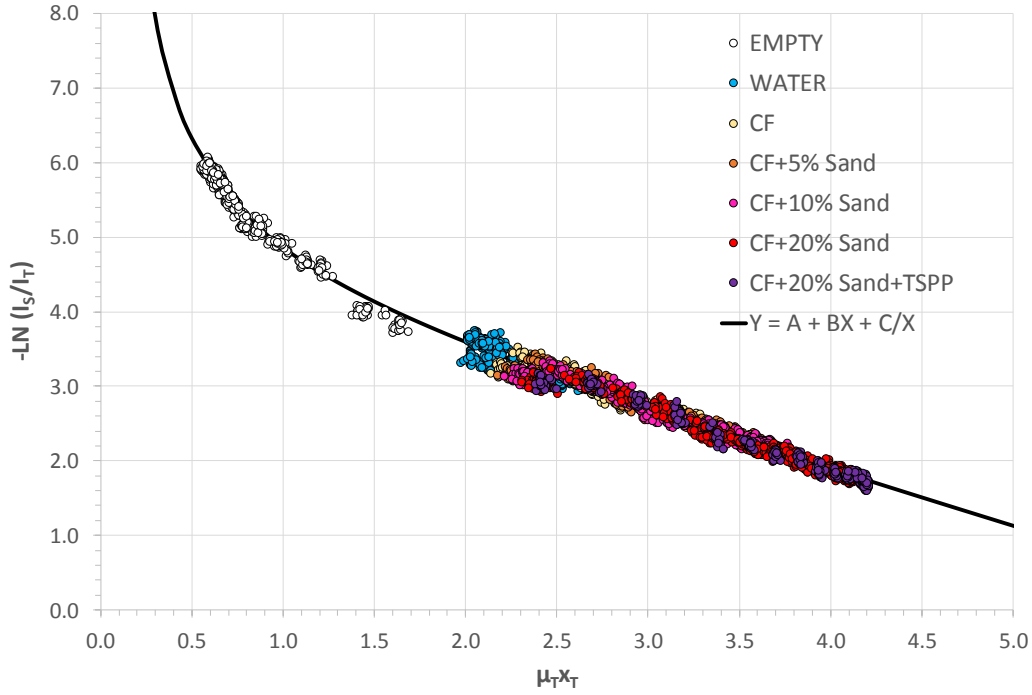

Figure 5. Normalized backscattering correction data for the high attenuation slurry measurements with the SRC GRT.

The results show that plotting the backscattering data in this way provides a reasonably good fit to the experimental data. A best-fit correlation to the data has been proposed below in Equation 6:

$$Y = A + BX + C/X \tag{6}$$

Where:

$Y = -ln(I_{S,i}/I_{T,i}) =$ natural logarithm of the ratio of scattered to attenuated radiation intensities
$X = \mu_T x_T = \sum \mu_j x_j = \mu_{slurry} x_{slurry} + \mu_{pipe} x_{pipe} =$ total attenuation in measurement volume
$A = 4.4610$
$B = -0.7110$
$C = 1.1094$

Note that the value for the independent parameter (X) in the correlation can be determined from the attenuated slurry + pipe intensity measurements according to the Beer-Lambert Law:

$$X = \mu_{slurry+pipe} x_{slurry+pipe} = -ln\left(\frac{I_{T,i}}{I_{0,i}}\right) \quad (7)$$

The correlation in Equation 6 also properly describes the expected backscattering behaviour outside of the experimental data range. As the attenuation (X) goes to zero, the trend goes to infinity (and thus the amount of backscattering goes to zero). This makes physical sense as no backscattering would exist without any attenuating material present. Similarly, as the attenuation (X) increases, so does the amount of backscattering. In this case, the backscattering intensity approaches the transmitted intensity as the attenuation becomes very high. As a practical limit the correlation is only valid for $X \leq$ 6.5 (the x-intercept). For X > 6.5 a value of Y = 0.01 has been chosen as the limit. This ensures that the backscattering intensity never exceeds the attenuated slurry + pipe intensity.

By correlating the data in this way, the backscattering intensity at each detector can be calculated from the measured slurry + pipe attenuated or transmitted intensity and a prior measurement of the unattenuated radiation intensity (in air with no pipe). In the development of the correlation, the measured attenuated intensities were obtained from the single source shutter open measurements described in Section 3.3 (steps (e) to (i)). However, during typical operation of the GRT, the shutters on all of the sources would be open when collecting measurement data (step (c)). Each of these attenuated intensity measurements will have both a transmitted and backscattered intensity component (whereas the attenuated intensity, $I_{T,i}$, used to develop the correlation in Equation 6 contains no backscattering contribution). In order to obtain the true attenuated intensity (with no backscattering component), the backscattering intensity must be calculated using an iterative approach. This true attenuated intensity is then used in the post-processing of the data to produce reconstructed tomograms (i.e. solids concentration distributions).

5 CONCLUSIONS AND RECOMMENDATIONS

The Gamma-ray Tomography unit (GRT) at the SRC Pipe Flow Technology Centre™ has been used to measure the solids concentration distributions from the reconstructed tomograms of high density clay/sand/water slurries in pipeline flow. To increase the accuracy of the reconstructed tomograms, and reduce the error from backscattered radiation, a method to determine the amount of backscattering in the measured signals at each detector for high attenuation slurries was required.

An improved semi-empirical backscatter correlation for the SRC GRT has been developed. It was found that the fraction of the measured attenuated signal related to backscattered radiation increases significantly with increasing signal attenuation (i.e. increased material density and/or path length). The correlation is similar in form to the Beer-Lambert Law and allows the backscatter contribution at each detector, and the true attenuated or transmitted intensities, to be calculated using an iterative approach from the measured uncorrected attenuated radiation intensities. Currently this correlation is only appropriate for homogeneous systems (i.e. uniform solids concentration distributions); however, testing is currently underway to expand the applicability to heterogeneous slurry systems.

ACKNOWLEDGEMENTS

This work was conducted as part of a Joint Industry research project at the SRC Pipe Flow Technology Centre™ funded primarily by the oil sands mining members of COSIA (Canada's Oil Sands Innovation Alliance) with contributions from Paterson & Cooke USA, Ltd. Contributions by the technical representatives to this research are gratefully acknowledged and the authors thank the sponsoring companies for supporting this work. The authors would also like to acknowledge the efforts of the SRC staff working on the project: A. Gossner, C. Knops, I. Betz, D. Kong, D. Riley, P. Schergevitch and L. McGilp. Without their tireless efforts this work could not have been completed.

REFERENCES

JOHANSEN G A, FRØYSTEIN T, HJERTAKER B T, OLSEN Ø, (1996), A dual sensor flow imaging tomographic system, Meas. Sci. Technol., 7, pp. 297-307

MAAD R, HJERTAKER B T, JOHANSEN G A, (2008), Semi-empirical correction model for high speed gamma-ray tomography, Meas. Sci. Technol., 19, 6pp

MOSOROV V, JOHANSEN G A, MAAD R, SANKOWSKI D, (2011), Monte Carlo simulation for multi-channel gamma-ray process tomography, Meas. Sci. Technol., 22, 10pp

PERRY R H, GREEN D W, (1997), *Perry's Chemical Engineers' Handbook*, 7th Ed., McGraw-Hill, New York, ISBN: 0-07-049841-5

SHOOK C A, ROCO M C, (1991), *Slurry Flow: Principles and Practice*, Butterworth-Heinemann, Boston, ISBN: 0-7506-9110-7

SPELAY R B, (2007), Solids Transport in Laminar, Open Channel Flow of Non-Newtonian Slurries, Ph.D. Thesis, University of Saskatchewan, Canada, pp. 65-67

SPELAY R B, GILLIES R G, HASHEMI S A, SANDERS R S, (2016), Effect of Pipe Inclination on the Deposition Velocity of Settling Slurries, Canadian Journal of Chemical Engineering, 94 (6), pp. 1032-1039

SPELAY R B, GILLIES R G, HASHEMI S A, SANDERS R S, (2017), Kinematic friction of concentrated suspensions of neutrally buoyant coarse particles, Proc. Hydrotransport 20, Melbourne, Australia, 15pp

TJUGUM S A, JOHANSEN G A, HOLSTAD M B, (2003), A multiple voxel model for scattered gamma radiation in pipe flow, Meas. Sci. Technol., 14, pp. 1777-1782